

Interim Progress Report for CDFR Agreement Number 15-0214SA

GENOME EDITING OF *TAS4*, *MIR828* AND TARGETS *MYBA6/A7*: A CRITICAL TEST OF *XYLELLA FASTIDIOSA* INFECTION AND SPREADING MECHANISMS IN PIERCE'S DISEASE

Principal Investigator:

Chris Rock
Texas Tech University
Dept of Biological Sciences
Lubbock, TX 79409-3131
chris.rock@ttu.edu

Cooperator:

Leo De La Fuente
Auburn University
Dept Entomology Plant Pathology,
Auburn, AL 36849
lzd0005@auburn.edu

Cooperator:

David Tricoli
University of California, Davis
Plant Transformation Facility
Davis, CA 95616
dmtricoli@ucdavis.edu

Research Associate:

Sunitha Sukumaran
Texas Tech University
Dept of Biological Sciences
Lubbock, TX 79409-3131
sunitha.sukumaran@ttu.edu

Graduate Research Asst:

Md. Fakhrul Azad
Texas Tech University
Dept of Biological Sciences
Lubbock, TX 79409-3131
fakhrul.azad@ttu.edu

Research Associate:

Sy Mamadou Traore
Auburn University
Dept Entomology Plant Pathology,
Auburn, AL 36849
traorsm@auburn.edu

Reporting Period: The results reported here are for work conducted from March 1, 2017- July, 2017.

INTRODUCTION

The most damaging effect of PD other than death of the vine is the reduction of production and shriveling of fruits. Our working model of PD etiology postulates microRNA828 (miR828) and evolutionarily-related *Trans-Acting Small-interfering locus4* (*TAS4*) activities silence target *VvMYBA6/A7* and other homologous *MYB* targets' expression in response to *Xylella fastidiosa* (XF) infection, mediated through inorganic phosphate (P_i) known in other species to regulate miR828 and other miRNA expressions^{1,2}. New deep sequencing transcriptome- and small RNA-Seq datasets were characterized in the March 2017 Interim Progress Report, data-driven results which validated miR828 as target and identified other phosphate-regulated miRNAs (miR827, miR399) as additional nodes in a network of miRNA and phased, small-interfering RNA (phasiRNA) effectors of PD etiology. We showed up-regulation of *vvi-miR399ig* and mis-regulation of downstream *PHT1;4L* family members by XF, and significant up-regulation of Major Facilitator Superfamily/SPX supporting the notion that phosphate homeostasis is key to XF disease etiology via phosphate-regulated miR828, -827, and -399. Other independent evidence supports our hypothesis: overexpression in Arabidopsis of Secreted Aster Yellows phytoplasma strain Witches' Broom Protein11 (SAP11) suppresses plant defense responses by triggering accumulation of cellular P_i ³. This result is consistent with observed increased expression of P_i starvation-induced miRNAs and altered P_i in XF-infected samples, described in prior progress reports. We found additional compelling evidence in the literature supporting our phosphate-regulation XF etiology model: in Arabidopsis infected with XF, genome-wide transcriptome analysis showed *TAS4* siRNA target *MYB PRODUCTION OF ANTHOCYANIN PIGMENT1/MYB75* and another phosphate-regulated locus, At5g20150/SPX DOMAIN, which is a positive regulator of cellular responses to phosphate starvation and subject to miR827 regulation^{1,4,6}, are both strongly down regulated by XF infection⁷. Furthermore, mis-regulation of *VvSPX1* and grapevine phosphate transporter *VvPHT2;1* subject to miR399 regulation^{6,8} are significantly down-regulated eight weeks after XF infection⁹.

We have generated strong evidence from our mRNA-Seq, sRNA-Seq and degradome datasets from XF-infected grape and tobacco materials, quantitation of xylem sap phosphate in PD-infected canes, and disease severity correlations with molecular phenotypes from greenhouse XF challenge experiments that support a refined

model whereby XF uses host small RNAs as a 'trojan horse.' This model serves as a paradigm to investigate not only phosphate as diffusible signal for synthesis of host polyphenolic anti-bacterial metabolites in PD etiology, but also the pleiotropic PD traits of berry shriveling, "green islands" (irregular lignification of bark) and "matchstick petioles," (abnormal abscission at petiole/leaf blade junctions)¹⁰. Many of the top-listed significantly differentially regulated *PHAS* and *TAS* genes described in the Mar. 2017 progress report are known effectors (Leucine-Rich-Repeat receptors, LRRs) of plant pathogen responses mediated by miRNA activities^{2, 11}. Systems analyses showed significantly different, and most importantly, *inverse* changes of mRNA and siRNA expressions¹² for secondary metabolism (specifically flavonoid/flavonol and anthocyanin) genes in XF-infected 2015 field samples from 'Calle Contento' Temecula vineyard compared to controls. This inverse relationship is interpreted to be functionally significant, whereby secondary (polyphenolics) metabolism is impacted by upstream hierarchical activation of negative regulators miR828 and *TAS4* siRNAs, which results in altered (decreased) phasiRNAs and up-regulation of mRNA templates of the phasiRNAs. Direct demonstration of altered expression by XF of the causal effector (miR828) for the regulatory MYB/anthocyanin cascade is a significant insight that strengthens our conclusions supporting the working model. Such clustering of gene ontology for disease resistance loci in our RNA-Seq, sRNA, and degradome datasets **very strongly support the working model** that XF infection modulates phasiRNA production and miRNA activities known to control pathogen resistance, in addition to *MIR828/TAS4*.

We are also taking a complimentary "overexpression" approach in tobacco to directly test the MYB-anthocyanins-as-XF-effectors hypothesis. The surrogate tobacco XF infection system developed by the Cooperator (De La Fuente)¹³ is being employed to more quickly assess susceptibility to XF infection of a transgenic tobacco line¹⁴ (Myb237) that over-expresses the Arabidopsis orthologue of VvMYBA6/A7: *PRODUCTION OF ANTHOCYANIN PIGMENT2/MYB90/PAP2*. We repeated the greenhouse XF challenge experiment on MYB overexpression genotypes and reported in the March 2017 progress report our confirmatory findings in support of the working hypothesis and results presented in the Feb. 2016 progress report. Here we present further quantitative and qualitative molecular analyses of deep sequencing small RNA libraries from both tobacco XF challenge experiments.

OBJECTIVES (as funded)

- I.** Demonstrate the efficacy of CRISPR/Cas9 transgenic technology for creating deletion mutants in *MIR828*, *TAS4*, and target *MYBA6/7*. When validated, future experiments will critically test these genes' functions in PD etiology and XF infection and spreading.
- II.** Characterize tissue-specific expression patterns of *TAS4* and *MIR828* primary transcripts, sRNAs, and *MYB* targets in response to XF infections in the field, and in the greenhouse for tobacco transgenic plants overexpressing *TAS4* target gene *AtMYB90/PRODUCTION OF ANTHOCYANIN PIGMENT2*.
- III.** Characterize the changes in (a) xylem sap and leaf inorganic phosphate (Pi), and (b) polyphenolic levels of XF-infected canes and leaves. (c) Test on tobacco in the greenhouse and XF growth *in vitro* the Pi analogue phosphite as a durable, affordable and environmentally sound protectant/safener for PD.

DESCRIPTION OF ACTIVITIES CONDUCTED TO ACCOMPLISH OBJECTIVES

- I. Test the miR828, *TAS4*, and target MYBA6/7 functions in PD etiology and XF infection and spreading by genome editing using CRISPR/Cas9 transgenic technology**

Fig. 1 shows good progress on regeneration of somatic embryo transformations of grapevine rootstock 101-14 initiated on 2/8/2017 and 2/15/2017. The Cooperator is spreading these cultures out at lower density to promote elongation, and observing candidate regenerants for anthocyanin phenotypes which would be de facto evidence of target gene editing. Experiments proposed on parallel transformation/regeneration of rootstock

'1103-P' have not been initiated, pending results of editing assays on regenerated 101-14 plants, which are anticipated to be received in Nov. 2017.

With successful production by the Cooperator (Tricoli, see Mar. 2017 progress report) of transgenic tobacco plants expressing the *MIR828/TAS4/MYB* CRISPR/Cas9 genome-editing vectors, another tool becomes available to test editing activity on endogenous *Nt-MIR828/TAS4/MYB* targets of our grapevine CRISPR vectors in a heterologous system. Here we report preliminary analyses of these transgenic materials in lieu of grapevine editing assays, which await delivery of regenerated materials from the Cooperator (Tricoli). We reported in Oct. 2016 progress report an established deletion detection PAGE assay in our lab using a known 15 nt deletion of the phytochrome *PHYD-1* gene of *Arabidopsis* ecotype Wassilewskija (Ws-2)¹⁵. We mined the draft tobacco genomes

(<https://solgenomics.net/tools/blast/>) to evaluate the prospect that at least one of our synthetic guide vectors targeting grapevine candidate effectors

(documented in Mar. 2016 progress report) could function to target the endogenous tobacco *Nt-MIR828a* and possibly *Nt-TAS4a,-b* loci. The *Nt-MYBs* (there are two; *NtAN2/ FJ472647.1* and *SGN-U375014*) are not expected to be targeted by grapevine synthetic guide RNAs. The essential requirements of *Streptococcus pyogenes* nuclease Cas9 are for both a Proximal Adjacent Motif 'NGG' 3' to the guide sequence, and perfect guide sequence match to the 'seed' region (nucleotides 1-12)¹⁶. The *Vv-MIR828** guide has a mismatch at guide seed position 9 of *Nt-MIR828a*. The *Vv-TAS4a* guide that targets the functional tasi-RNA 3'D4(-) species has a mismatch at nt 11 to both *Nt-TAS4a* and *-TAS4b*, however the Proximal Adjacent Motif NGG is absent (data not shown). Preliminary results of a PAGE assay on regenerated tobacco transgenic for the *VvTAS4ab*, *VvMYBA6*, and *VvMYBA7* editing vectors were negative (data not shown). We will also test the *VvMIR828* editing vector regenerated transgenic tobacco lines for evidence of Cas9 editing activity on *NtMIR828ab* going forward.

Summary of accomplishments and results, Objective I. We are on track to complete the production of deliverable transgenic grapevines this calendar year. Validation of editing events and characterization of editing efficiencies going forward will be performed on future regenerated grapevines by PCR cloning and sequencing of target genes, and PAGE-based genotyping.

II. Characterize tissue-specific expression patterns of *TAS4* and *MIR828* primary transcripts, siRNAs, and *MYB* targets in response to XF infections in the field, and in the greenhouse for tobacco transgenic plants overexpressing *TAS4* target gene *AtMYB90/PRODUCTION OF ANTHOCYANIN PIGMENT2*.

In the previous progress reports and the 2016 PD-GWSS Symposium we characterized and correlated molecular phenotypes of XF titres, *TAS4*-3'D4(-) siRNA and miR828 abundances by RNA blot, and anthocyanin quantities extracted from the transgenic tobacco line Myb237 overexpressing *AtMYB90* challenged with XF in the greenhouse, and from PD-infected and symptomless Merlot leaves and petioles collected from the 'Calle

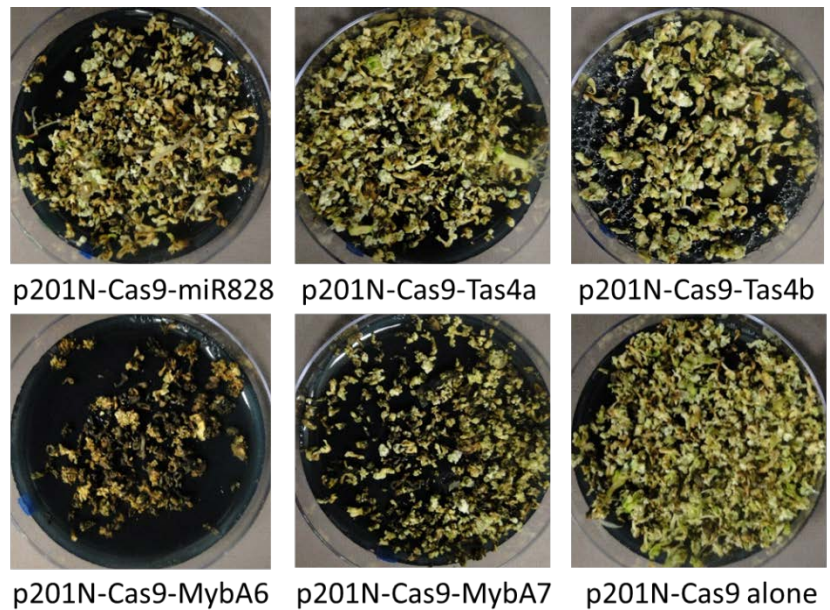


Fig. 1. Progress of regeneration of grapevine transformants of p201-N-Cas9 vector constructs harbored in Cooperator-sourced EHA105 *Agrobacterium* strain initiated Feb. 2017, showing good response.

Contento' vineyard in Temecula CA, and the Black Stock vineyard in Dahlonega, Lumpkin Co., GA. Those compelling results and preliminary analyses of our first and second Illumina small RNA (and transcriptome, for grape) libraries generated from the same tobacco- and California XF-infected and control samples strongly support the working model of XF interaction with anthocyanin biosynthesis regulation by the host during PD progression. Systems analyses showed significantly different, and most importantly, *inverse* changes of mRNA and siRNA expressions for secondary metabolism genes in XF-infected 2015 field samples from 'Calle Contento' Temecula vineyard compared to controls (Mar. 2017 progress report). Results showed significant differences in accumulation of anthocyanins in XF-infected vs. control leaves from the field and greenhouse samples. Cooperator De La Fuente repeated the tobacco Myb237 XF challenge experiment in late 2016 and preliminary analyses of the repeat experiment support the previous observation of significantly greater (~50% of leaves) disease symptom development in homozygous (Hmo) MYB overexpressing lines five weeks after XF challenge. Results also showed a significant decrease in anthocyanins in XF-infected transgenics compared to buffer alone controls (Mar. 2017 progress report), suggesting a dynamic interaction between XF and host regulation of anthocyanin metabolism consistent with the working model. Lower normalized sRNA reads in homozygous transgenic genotype in response to XF supported findings by small RNA blot analysis that XF suppresses a conserved tobacco MYB90-TAS4 autoregulation activity¹⁷, strongly supporting the working hypothesis. It remains unclear at what level XF acts in the autoregulatory loop, or possibly higher up in a hierarchy of transcription factors, because interpretation is confounded by autoregulatory activity of either PAP2 or endogenous cognate MYBs.

We have quantified XF titres by qRT-PCR¹⁸ for the second tobacco experiment and the result is shown in **Fig. 2**. The similar XF titres in HMO-versus control SR1-infected samples permit us to correlate the observed greater disease severity in HMO versus either HMI or SR1 controls (Mar. 2017 progress report), further supporting our working hypothesis and validating the results of the 2015 experiment.

We continue to characterize the first Illumina TruSeq stranded degradome libraries^{20, 21} for discovery of the sRNA triggers of transitivity revealed by ShortStack²² and PhaseTank²³ softwares and are in process of generating biological replicate datasets from the June 2017 Calle Contento samples. This systems approach builds on the identified sRNA candidates and importantly will uncover genome-wide leads for other etiological effectors/reporters of PD and network analyses of gene interactions affecting primary and secondary metabolism and disease resistance mechanisms.

We have analyzed the sRNA datasets from the 2015-2016 tobacco XF-challenge experiments with the statistical software DESeq2²⁴ for computational identification of

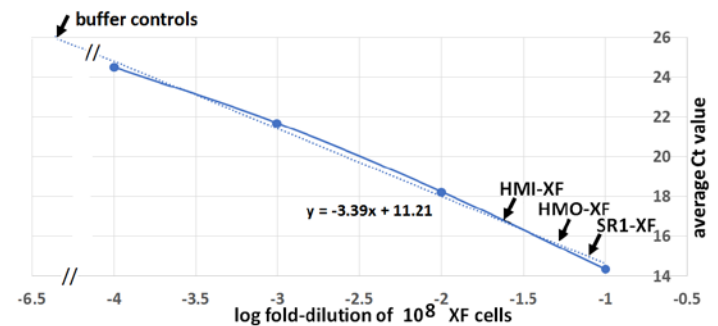


Fig. 2. Standard curve of XF titres in tobacco 2016 XF challenge repeat experiment. Arrows point to the equivalent numbers of cells in petiole samples, normalized to g fresh weight.

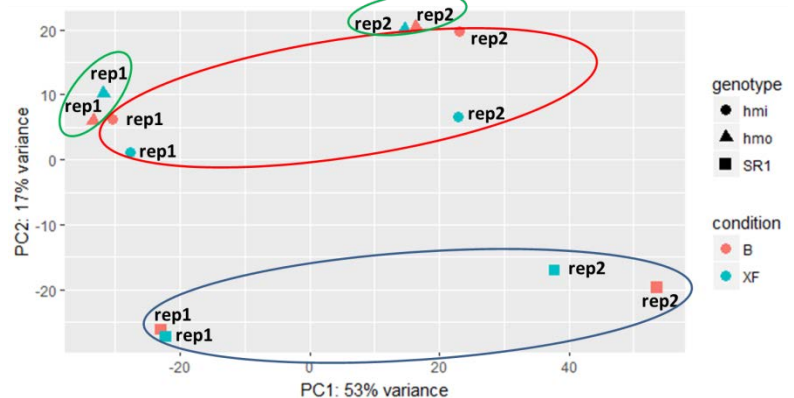


Fig. 3. Principal Component Analysis plot of technical (x-axis) and biological (y axis) replicate small RNA libraries made from 2015 and 2016 XF challenge experiments. Genotype sample clusters are enclosed by colored ovals: control (SR1; blue), hemizygous AtPAP2 (hmi; red) and AtPAP2 homozygous (hmo; green). This type of plot is useful for visualizing the overall effect of experimental covariates and batch effects.

differentially expressed clusters of small RNA-producing loci, focusing on *MIRNAs*. **Fig. 3** shows that the

Table I. Statistically significant mis-regulated miRNAs in XF-challenged control and transgenic tobacco expressing MYB AtPAP2. Down-regulated miRNAs are in bold .						
miRNAs, family	ShortStack Cluster #	Log ₂ FC, XF	<i>p</i> -adj*	mean reads/libr	Predicted targets [^]	Ref.
nta-miR156 b,b.2,c,d,f,h,g,i,j	4096304	1.93	0.00009	45	Squamosa-promoter binding Transcription factors SGN-U384021, SGN-U367182, SGN-U379394, SGN-U385631; phospholipase C SGN-U370298	[28]
	3462213	1.59	0.0002	27		
	2434188	1.41	0.0016	48		
	788779	1.71	0.0024	2		
	3376104	1.63	0.0032	2.4		
	1191746	1.29	0.0037	36		
	87354	1.27	0.0039	67		
	4099790	1.04	0.014	97		
	2549550	0.96	0.018	135		
Novel-49, -47	2923885	1.46	0.00014	22	Ribosomal S17/EMB1129 SGN-U366077, SGN-U386150	
	2798716	0.96	0.02	105		
Novel-13	804764	1.83	0.0006	10	two-pore calcium channel TPC1 SGN-U362916, regulatory protein NPR1 SGN-U366438	
nta-miR6154*	1816342	1.05	0.0013	99	Unknown protein SGN-U364841, inorganic pyrophosphatases SGN-U363803, SGN-U372048	
Novel-43	2513360	1.41	0.0018	23	Unknown protein FS400655, ubiquitin carrier TC153643	
Novel-35, -17, -25, -30	2100099	1.2	0.003	84	ras-related protein RABD2a SGN-U383967	
	902344	1.15	0.004	128		
	1470478	1.02	0.013	618		
	1815728	1.02	0.025	20		
nta-miR3627	3338070	1.91	0.008	3.2	Ca ²⁺ -ATPase SGN-U371584	[50]
nta-miR398b,c	606156	-1.01	0.009	537	rhodanese-like domain CDC25 phosphatase SGN-U367853	[27]
	3761333	-0.88	0.024	85		
stu-miR8036/482/21 18-like	4020631	1.40	0.015	7.2	F-box domain SKIP2/At5g67250-like SGN-U371093; arsenite anion-transporting ATPase SGN-U383925, SGN-U369282	
nta-miR6146b	1819435	0.74	0.02	313	beta-galactosidase SGN-U371035	
ptc-miR393b-like	1902585	1.06	0.02	17	Auxin co-receptors TIR1E3 ligase SGN-U383522, SGN-U370791	[33-35]
nta-miR319a	597095	1.39	0.04	82	LRR-extensin SGN-U382334; unknown proteins SGN-U371226, SGN-U381403	
nta-miR167e,d	3485917	1.00	0.04	19	homeobox-leucine zipper SGN-U364410; protein phosphatase2C SGN-U364430	[11]
	2931362	0.94	0.04	15		
Novel-65	3794016	0.81	0.05	22	Leucine-rich Repeat SGN-U369408	
nta-miR827a,b	3223767	1.07		16		[2]
	3482419	0.76		214		
nta-miR399a,f,f2,e,c	127533	-0.21		38	PHO2/ UBC24-like SGN-U383809 star: RNA binding protein47 SGN-U362949, SGN-U369270, SGN-U386806	[2]
	1176109	-0.21		14		
	127655	-0.14		16		
	176416	-0.08		18		
	1561612	-0.51		1.3		
nta-miR828a,b	3189162	-0.03		0.9	AtMYB30-like transcription factor SGN-U375014	[37]
	3041986	-0.21		4.9		
Nt-TAS4a,b	3109915	-0.09		8,297	NtAN2 MYB, FJ472647.1	[14, 37]
	2376596	-0.20		15,250		

* Benjamini-Hochberg family-wise corrected, based on 166 *MIRNAs* characterized from ShortStack output.

[^] from http://plantgrn.noble.org/v1_psRNATarget/ [26]

replicate experiments gave good concordant results in terms of small RNA locus signal reproducibility (datapoint clusters enclosed by colored ovals), where principle component 2 (y axis) is effectively genotype- and XF treatment- specific. Principal component 1 (x-axis) represents the technical/batch variation between 2015 and 2016 experimental replicates. We have identified with ShortStack²² about 50 novel miRNAs that meet the community standards for annotation²⁵, including sequencing a miRNA* species; a few of these novel miRNAs have multiple family members and conserved predicted targets²⁶. **Table I** shows the top miRNA leads that are significantly differentially expressed in XF-infected leaves in both replicate transgenic tobacco XF challenge experiments. Although not statistically significant, miR828ab and *TAS4ab* are down-regulated by XF challenge, as previously shown by sRNA blots in the Mar. 2017 progress report. In addition, miR398 is significantly down regulated by XF infection, as has been shown in Arabidopsis plants challenged with avirulent strains of *Pseudomonas syringae* that causes bacterial speck in the Solanaceae, such as Pst DC3000 *avrRpm1* and Pst DC3000 *avrRpt2*²⁷. miR827ab are up-regulated, and miR399 family members are all down-regulated, consistent with the working hypothesis and preliminary results of grapevine XF- and control sRNA libraries reported in the Mar. 2017 progress report. miR827 and miR399 are known phosphate homeostasis effectors shown to be mis-regulated in greening diseased citrus caused by the gram-negative *Liberibacter asiaticus*².

Interestingly, the targets of the most significantly up-regulated miRNA family, miR156, have been shown in Arabidopsis to negatively regulate anthocyanin biosynthesis whereby increased miR156 activity promotes accumulation of anthocyanins²⁸, supporting our working model. miR156 targets SPL9 which directly prevents expression of anthocyanin biosynthetic genes through destabilization of a MYB-bHLH-WD40 transcriptional activation complex²⁸, providing a direct link/mechanism for how VvMYBA6/7 and other miR828 MYB targets in grapevine are deranged by XF infection (prior progress reports) resulting in anthocyanin accumulation (see below). Another inference from studies in Arabidopsis is that SPL7 activates the transcription of both anthocyanin biosynthetic genes²⁹ and *MIR398*^{30,31}; our result showing down-regulation of miR398 (**Table I**) predicts that SPL7 grape and tobacco orthologs may be down-regulated by XF infection.

Imputation from results in tobacco to grapevine.

Table II shows results from mRNA-Seq analysis³² of grapevine XF versus healthy control analyses (see Mar. 2017 progress report) consistent with the above predictions. VvSPL5, SPL2, SPL10/11, SPL6-L, and SPL9 targets of miR156, and VvARF6/8 targets of miR167 are the top leads as significant down-regulated effectors of XF etiology in an upstream network hierarchy encompassing miR828 and other phosphate-regulated miRNAs, guided by

Table II. XF infection effects on expression of mRNAs targeted by miR156, miR398, miR167, and miR393. Data from RNA-Seq of CA Temecula samples (July 2015), imputed from results (Table I) of XF effects on tobacco miRNAs.

miRNA	Arabidopsis Annotation	orthologue	Mean reads/lib	mRNA L ₂ FC [†]	mRNA q-val [¶]
miR156	VIT_12s0028g03350	SPL5	32	-2.15	0.01
	VIT_11s0065g00170	SPL2	300	-0.61	0.02
	VIT_01s0010g03710	SPL10/11	56	-1.03	0.02
	VIT_01s0011g00130	SPL6-L	7	-1.38	0.10
	VIT_08s0007g06270	SPL9	39	-0.59	0.39
	VIT_01s0010g03910	SPL13	22	3.36	0.01
	VIT_10s0003g00050	SPL3	37	0.43	0.10
	VIT_17s0000g05020	SPL6	32	0.45	0.16
VIT_05s0020g02160	SPL7 [^]	660	-0.02	0.05	
miR398	VIT_01s0011g00830	PSMD10 [§]	3240	0.56	0.02
miR167	VIT_10s0003g04100	ARF6	124	-2.06	0.005
	VIT_04s0079g00200	ARF8	127	-0.86	0.02
	VIT_12s0028g01170	ARF6-L	171	-0.30	0.07
miR393	VIT_07s0104g01320	TIR1-L	303	-0.56	0.10
	VIT_14s0030g01240	TIR1-L	519	1.45	0.05
	VIT_14s0068g01330	TIR1-L	3340	0.70	0.07

¶ False Discovery Rate < 0.1; Benjamini & Hochberg multiple comparisons, Least Likelihood Ratio.

† XF infection LFC Wald test, kallisto/sleuth [32].

[^] not predicted to be miR156 target. miR156 targets SPL3-L, SPL13A-L not detected.

[§] 26S proteasome non-ATPase regulatory subunit 10 (PSMD10); predicted target of miR398* [26].

imputation from the tobacco results. These novel data-driven results drawing on model organisms further substantiate our claim that a complex miRNA regulatory network hierarchy coordinates expression of miR828/*TAS4* and other miRNAs important for PD etiology. Numerous reports have documented the up-regulation of auxin effectors miR393 and miR167 in response to biotic stresses^{11, 33-35}; we document in **Table I** similar results in response to XF infection and concordant inverse changes in target mRNAs (**Table II**). We are in the process of validating the differential expressions by sRNA blots and target mRNA cleavage activities of novel miRNAs by 5' modified RACE³⁶.

Although low base mean read depths for nta-*MIR828ab* and predicted MYB targets of miR828 (SGN-U375014) and *TAS4*-3'D4(-) (AN2) precludes conclusive evidence for their *significantly* different expressions in response to XF in tobacco, the trends are clear and compelling- XF infections in both tobacco and grape result in deranged miR828 and related miRNA expressions that impact target gene expressions (Mar. 2017 progress report; **Table II**). Based on strong correlations seen across other libraries previously analyzed³⁷, *Vv-TAS4c* is emerging as a likely causal effector for XF response. The diversity and conservation of phasiRNA and *MIRNA* loci across plant taxa revealed thus far by our results encompasses novel miRNAs, orthologues of *MYBs* triggered by miR828 in many species³⁸⁻⁴⁶, including grape⁴⁷, the *TAS* effectors *SUPPRESSOR OF GENE SILENCING3 (SGS3)* and *DCL2*^{42, 48} (Mar. 2017 progress report), and the huge family of Leucine-rich Repeat Receptors (*LRR*) targeted by ancient homologous miRNAs miR8036/482/2118^{38, 42, 49, 50} (**Table I**). Their collective loss in bacteria-infected tissues that results in susceptibility^{49, 51} supports their functions as master regulators targeted by XF.

Summary of accomplishments and results, Objective II. Our results for XF differentially regulated miRNAs in tobacco are completely novel. The working model for PD etiology by altered phosphate regulation of miR828/*TAS4* and *MYB* target genes is supported by our sRNA and RNA-Seq datasets. A highly correlated network of miRNA/phased siRNA-producing- and *TAS* noncoding loci known to function in plant immunity across plant taxa has been characterized. A transgenic tobacco model shows that XF infection modulates a conserved *TAS4* autoregulatory loop that we have extended to include *MIR828*, which correlates with PD symptom severity. A direct test of the model in grapevine (Obj. I) by genome editing of the positive and negative effector loci is well grounded now, based on our deep sequencing evidence for miR828/*TAS4* roles in PD. Once transgenic grapevine materials are available, deep sequencing libraries will be constructed of control and XF-challenged genotypes and characterized in reference to our current baseline results.

III. Characterize the changes in (a) xylem sap and leaf P_i , and (b) polyphenolic levels of XF-infected canes and leaves. (c) Test on tobacco in the greenhouse and XF growth in vitro the P_i analogue phosphite as a durable, affordable and environmentally sound protectant/safener for PD.

(a) Leaf $[P_i]$. Prior results of Cooperator (DLF)¹³ show strong associations of elemental P decreases with XF infection of many host species, however the biological complexities of P (e.g. phosphoproteins, lipids, nucleic acids, subcellular compartmentation, etc) precludes conclusive interpretation of those existing data. In the Oct. 2016 progress report we showed by ion chromatography-flame ionization detection (IC-FID)⁵² an unexpectedly

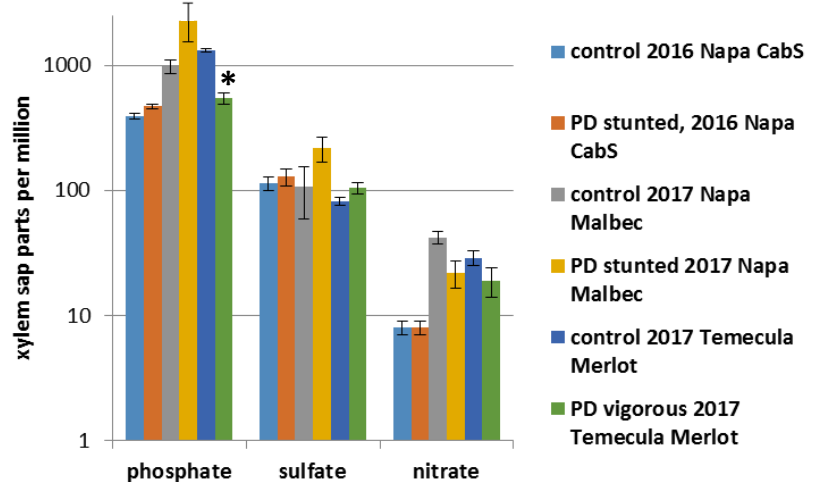


Fig. 4. Quantitation of xylem sap inorganic ion concentrations from healthy and PD symptomatic canes collected from three sites and varieties over two years. Asterisk (*) indicates significantly different from control, $P < 10^{-8}$.

higher concentration of P_i in XF-infected Cab Sauv canes from Napa CA. However, in those initial PD samples from May 2016 we observed severe stunting, making side-by-side comparisons with healthy control canes confounded as xylem sap extraction was quantitatively and qualitatively different for the smaller infected canes versus controls. Results from a second set of xylem sap samples from an adjacent block of Malbec vines collected from Napa in May, 2017 is shown in **Fig 4**. The results corroborate the original observation of higher trend of $[P_i]$ in the PD-infected, stunted canes. However, it was realized after collection that an inadvertent variable had been introduced in those N. CA samples from 2016/17: because of the local viticulture practice of decapitation of the cordon/crown for PD-infected vines, the test samples were taken from PD symptomatic suckers emerging from the rootstock, which is a different genotype and developmental growth habit from the control samples, further confounding the interpretation. Therefore, more appropriate samples were obtained in a subsequent collection of materials from Calle Contento vineyard, Temecula CA in June, 2017 where the Merlot variety leaves and canes from PD symptomatic vine samples were not developmentally stunted, allowing an appropriate side-by-side comparison controlled for genotype and developmental state. **Results in Fig. 4 show, as originally hypothesized, that comparable PD-infected canes have significantly lower P_i concentrations in xylem sap than healthy controls.** We have petiole samples from each independent cane assayed, and we are assaying XF titers in subtending leaf petioles to directly correlate with P_i for cane xylem sap.

In vivo nuclear magnetic resonance (NMR) permits analysis of subcellular $[P_i]$ that can provide insight into XF perturbation of host physiology. The 2016 fresh leaf samples from Temecula Calle Contento Merlot vineyard were used for pilot experiments to assess the suitability of NMR quantitation⁵³ of P_i in whole leaf disks, in collaboration with Dan Borchardt, Dept of Chemistry, UC-Riverside. **Fig. 5** shows the results of the analysis on developmentally normal (large) PD-infected leaves, which supports the data in **Fig. 4** for matched developmental states correlating a ~59% decrease in xylem sap $[P_i]$ with ~67% decreased leaf disk intracellular P_i (normalized per leaf disk). The vertical amplitude corresponds closely to the number of atoms with a particular frequency. The frequency shift corresponds to the chemical environment. The presumed major band ($\delta \sim 1-5$ ppm) is interpreted as a combination of cytosolic plus vacuolar P_i ; band broadening precluded definitive designation, but differences in chemical shifts between control and diseased samples indicated cytosolic P_i (downfield chemical shift)⁵³ is disproportionately affected by PD. Characterization of other energy status molecules like sugar-phosphates, ATP/ADP, and NADP was not possible due to broadened bandwidths, anaerobic conditions, and small sample sizes/acquisition times, but the upfield chemical

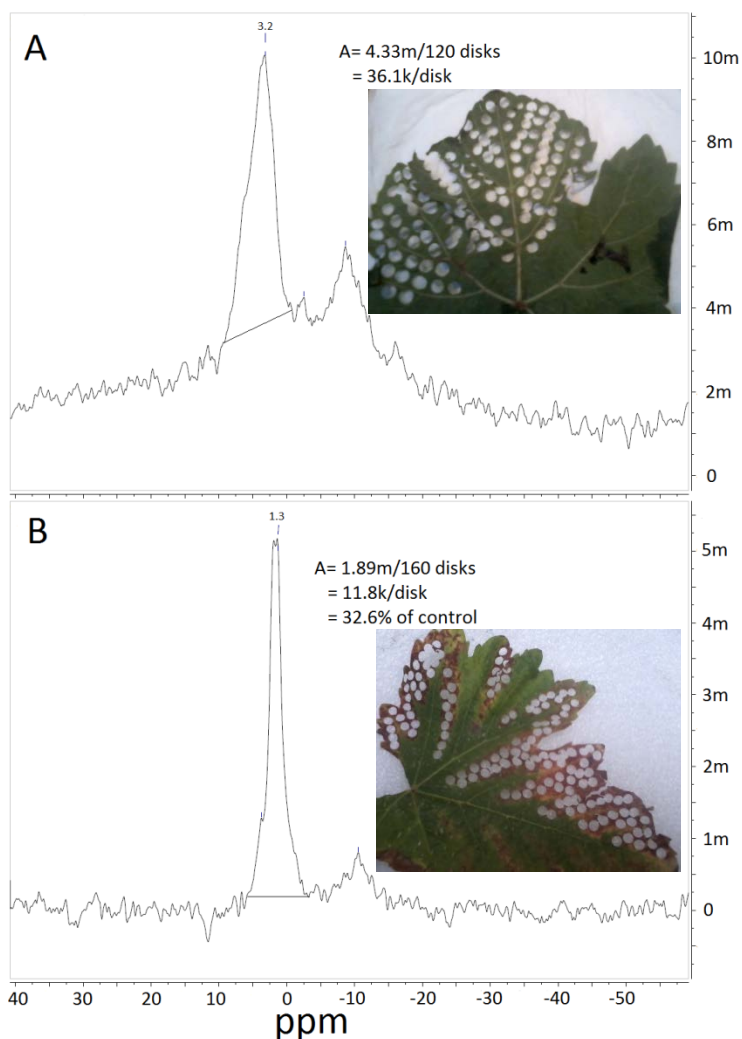


Fig. 5. NMR of ^{31}P quantity (Area, A/disk) and quality (δ , parts per million, ppm) in 5mm leaf disks (insets) of (A) healthy and (B) XF- infected leaf from Calle Contento vineyard collected August 2016. Data from 256 scans acquired with Broadband Observe probe at 242.938MHz on a Bruker Avance 600, Analytical Chemistry Instrumentation Facility, UC-Riverside, courtesy of Dan Borchardt. δ values relative to external reference 85% H_3PO_4 using unlocked D_2O drift compensation.

shift of the major band (P_i) in infected samples (Fig. 3B) suggests that this is the vacuolar P_i signal (pH~5.5) whereas the downfield P_i signal corresponds to cytoplasmic P_i (pH ~7) as expected in healthy leaf disks (Fig. 3A). Taken together, these results support our working hypothesis that XF infection causes a significant decrease in **leaf and xylem** sap P_i concentrations.

(b) Polyphenolics in XF-infected canes and leaves. We previously reported preliminary results for identification in leaf extracts from CA and GA field samples of anthocyanins cyanidin, delphinidin, and malvidin by Select Reaction Monitoring (SRM) High Performance Liquid Chromatography-Mass Spectrometry (HPLC-MS)(Oct. 2015 and 2016 progress reports). Samples are run on an Acclaim Pepmap RSLC 75 μm x 15 cm nanoViper C18 2 μm column with 95% water:formic acid as stationary phase and 100% acetonitrile as mobile phase, linear gradient from 5-100% mobile in 30'. The method entails specifying the parent mass of the compound for tandem MS|MS fragmentation and then specifically monitoring for fragment ion(s) representing the aglycone species. We have employed the method to quantify anthocyanins in xylem sap from the Temecula June 2017 field samples and report in **Table III** the preliminary results for quantification of cyanin and malvin. The results are consistent with the hypothesis that XF infection results in accumulation of anthocyanins in xylem sap. Similar results have been reported for procyanidins and other polyphenolics two months post-XF infection in Thompson seedless and several winegrape cultivars^{54,55}. Phenolic levels in Merlot xylem sap correlate with PD severity compared to other cultivars⁵⁶. Taken together these results support our working hypothesis that the xylem sap anthocyanins and other polyphenolics are important for PD disease progression.

Table IV shows the results of anthocyanin quantification from the most recent leaf sample collection in late June, 2017 from Calle Contento vineyard, Temecula CA (see **Fig. 4** result for concordant cane xylem sap ionomics) compared to prior results from 2015. The results continue to support the working hypothesis. We are in the process of quantifying XF titers in concordant petioles samples from these leaf and cane samples by RT-PCR (**Fig. 2**), repeating the quantification of anthocyanins in 2015, 2016, and 2017 field samples, and preparing sRNA and mRNA-Seq libraries (Obj. II) from these most recently collected samples. Going forward, the analyses will be combined with existing sRNA, mRNA-Seq and degradome library results from 2015 and 2016 field samples and those statistically defensible results from these three biological replicate experiments will be published.

Table III. Quantification of cyanin and malvin anthocyanins in xylem sap from Temecula CA 2017 samples by Select Reaction Monitoring (SRM) High Performance Liquid Chromatography-Mass Spectrometry.

Sample	nmoles cyanidin/vol	nmoles malvin/vol
XF-infected vine sap	0.44 (±0.19)	3.18 (±0.83)
Healthy control sap	n.d.	n.d.

Table IV. Correlation of anthocyanins with XF titres in PD and control Merlot leaves and petioles from Temecula CA in 2015 versus 2017

Sample	XF titre (CFU/gfw)	μmoles cyanidin-O-Glu/mgfw equivalents (± s.e.m.)	
		2015*	2017
XF-infected vines	1.4 x 10 ⁸	74.4 (±12.6)	1.37 (±0.01)
Control vines	1 x 10 ⁴	13.7 (± 4.6)	0.05 (±0.01)
P value		< 0.02	0.0001

* different spectrophotometer than used in 2017; re-calibration warranted

(c) P_i analogue phosphite as effector of XF growth and safener of disease symptoms. The Cooperator (De La Fuente) has provided XF Temecula-1 and WM-1 strains to the PI and shared best practices for XF microbiological methods during a site visit by Dr. Sukumaran to Auburn GA in May, 2017. Our attempts to date to assess phosphite effects on XF growth rates in liquid culture have been hampered by difficulty quantifying growth rates due to attendant intrinsic variation associated with slow growth (the scientific name of XF translates as 'difficult to please'). We are currently developing a plate growth assay in lieu of a liquid culture method. If results are positive, safener treatments of tobacco and grapevine under greenhouse XF challenge will follow.

Summary of accomplishments and results, Objective III. Together with *MIRNA* genes and target effectors of phosphate homeostasis revealed from Objective II, we have direct evidence for xylem sap inorganic phosphate (Pi) involvement in PD that further substantiates the working hypothesis.

PUBLICATIONS PRODUCED

Rock, C.D. (April, 2017) "Phenylpropanoid metabolism." Invited review. *Encyclopedia of Life Science*. Chichester, UK: John Wiley and Sons. <http://www.els.net/WileyCDA/ElsArticle/refId-a0001912.html>. DOI: 10.1002/9780470015902.a0001912.pub2

RESEARCH RELEVANCE STATEMENT

The PD-GWSS Board has suggested knocking out genes involved in diffusible signals and host chemical specificity for PD etiology by CRISPR/Cas9. This project endeavors to meet that mandate by knocking out *MIR828*, *TAS4*, and *TAS4* targets *MYBA6/7*, characterization of phosphate imbalances caused by XF, and whether phosphite applications can function as a 'safener' to impact PD etiology.

LAYPERSON SUMMARY OF PROJECT ACCOMPLISHMENTS

Our proof-in-principle experimental results to date are impacting understanding host-vector-pathogen interactions in PD. We continue efforts to critically test the XF infection/spread-via-host-miRNA-derangement hypothesis directly by "knocking out" the key hypothesized *MIR828/TAS4/MYB* genes using a new genome editing technology- Clustered Regularly Interspaced Short Palindromic Repeats (CRISPR/Cas9)^{57, 58} that the CDFA-PD Board nominated as a feasible, high-priority approach to engineering PD resistance. The transgenic grapevines are on track to be regenerated and made available by the Cooperator (Tricoli) for further characterization by November, 2017.

STATUS OF FUNDS

Funds are on track to be used by the end of the no-cost extension (Dec., 31, 2017).

SUMMARY AND STATUS OF INTELLECTUAL PROPERTY ASSOCIATED WITH PROJECT

We still await the Examiner's response to the PI's USPTO patent application #13/874,962 response filed October 18, 2016.

LITERATURE CITED

References

1. Hsieh LC, Lin SI, Shih ACC, Chen JW, Lin WY, Tseng CY, Li WH, Chiou TJ. (2009) **Uncovering small RNA-mediated responses to phosphate deficiency in Arabidopsis by deep sequencing.** *Plant Physiol* **151**: 2120-2132
2. Zhao H, Sun R, Albrecht U, Padmanabhan C, Wang A, Coffey MD, Girke T, Wang Z, Close TJ, Roose M, Yokomi RK, Folimonova S, Vidalakis G, Rouse R *et al.* (2013) **Small RNA profiling reveals phosphorus deficiency as a contributing factor in symptom expression for citrus Huanglongbing disease.** *Mol Plant* **6**: 301-310
3. Lu Y-T, Li M-Y, Cheng K-T, Tan CM, Su L-W, Lin W-Y, Shih H-T, Chiou T-J, Yang J-Y. (2014) **Transgenic plants that express the phytoplasma effector SAP11 show altered phosphate starvation and defense responses.** *Plant Physiol* **164**: 1456-1469
4. Lin W-Y, Huang T-K, Chiou T-J. (2013) **NITROGEN LIMITATION ADAPTATION, a target of microRNA827, mediates degradation of plasma membrane-localized phosphate transporters to maintain phosphate homeostasis in Arabidopsis.** *Plant Cell* **25**: 4061-4074

5. Lin S-I, Santi C, Jobet E, Lacut E, El Kholti N, Karlowski WM, Verdeil J-L, Breitler JC, Périn C, Ko S-S, Guiderdoni E, Chiou T-J, Echeverria M. (2010) **Complex regulation of two target genes encoding SPX-MFS proteins by rice miR827 in response to phosphate starvation.** *Plant Cell Physiol* **51**: 2119-2131
6. Park BS, Seo JS, Chua N-H. (2014) **NITROGEN LIMITATION ADAPTATION recruits PHOSPHATE2 to target the phosphate transporter PT2 for degradation during the regulation of Arabidopsis phosphate homeostasis.** *Plant Cell* **26**: 454-464
7. Rogers EE. (2012) **Evaluation of *Arabidopsis thaliana* as a model host for *Xylella fastidiosa*.** *Mol Plant-Microbe Interact* **25**: 747-754
8. Hackenberg M, Shi B-J, Gustafson P, Langridge P. (2013) **Characterization of phosphorus-regulated miR399 and miR827 and their isomirs in barley under phosphorus-sufficient and phosphorus-deficient conditions.** *BMC Plant Biol* **13**: 214
9. Choi H-K, Iandolino A, da Silva FG, Cook DR. (2013) **Water deficit modulates the response of *Vitis vinifera* to the Pierce's disease pathogen *Xylella fastidiosa*.** *Mol Plant-Microbe Interact* **26**: 643-657
10. Stevenson JF, Matthews MA, Rost TL. (2005) **The developmental anatomy of Pierce's Disease symptoms in grapevines: green islands and matchsticks.** *Plant Dis* **89**: 543-548
11. Li Y, Zhang QQ, Zhang JG, Wu L, Qi YJ, Zhou JM. (2010) **Identification of microRNAs involved in pathogen-associated molecular pattern-triggered plant innate immunity.** *Plant Physiol* **152**: 2222-2231
12. Usadel B, Poree F, Nagel A, Lohse M, Czedik-Eysenberg A, Stitt M. (2009) **A guide to using MapMan to visualize and compare Omics data in plants: a case study in the crop species, maize.** *Plant Cell Environ* **32**: 1211-1229
13. De La Fuente L, Parker JK, Oliver JE, Granger S, Brannen PM, van Santen E, Cobine PA. (2013) **The bacterial pathogen *Xylella fastidiosa* affects the leaf ionome of plant hosts during infection.** *PLoS ONE* **8**: e62945
14. Velten J, Cakir C, Youn E, Chen J, Cazzonelli CI. (2012) **Transgene silencing and transgene-derived siRNA production in tobacco plants homozygous for an introduced *AtMYB90* construct.** *PLoS ONE* **7**: e30141
15. Aukerman MJ, Hirschfeld M, Wester L, Weaver M, Clack T, Amasino RM, Sharrock RA. (1997) **A deletion in the *PHYD* gene of the *Arabidopsis* Wassilewskija ecotype defines a role for phytochrome D in red/far-red light sensing.** *Plant Cell* **9**: 1317-1326
16. Wu X, Kriz AJ, Sharp PA. (2014) **Target specificity of the CRISPR-Cas9 system.** *Quant Biol* **2**: 59-70
17. Luo Q-J, Mittal A, Jia F, Rock CD. (2012) **An autoregulatory feedback loop involving *PAP1* and *TAS4* in response to sugars in *Arabidopsis*.** *Plant Mol Biol* **80**: 117-129
18. Expert Working Group, European and Mediterranean Plant Protection Organization Panel on Diagnostics in Bacteriology. (2016) **Protocol PM 7/24 (2), *Xylella fastidiosa*.** *European and Mediterranean Plant Protection Organization (EPPO) Bulletin* **46**: 463-500
19. Francis M, Lin H, Rosa J-L, Doddapaneni H, Civerolo E. (2006) **Genome-based PCR primers for specific and sensitive detection and quantification of *Xylella fastidiosa*.** *Eur J Plant Pathol* **115**: 203-213
20. Addo-Quaye C, Eshoo TW, Bartel DP, Axtell MJ. (2008) **Endogenous siRNA and miRNA targets identified by sequencing of the *Arabidopsis* degradome.** *Curr Biol* **18**: 758-762
21. German MA, Pillay M, Jeong DH, Hetawal A, Luo SJ, Janardhanan P, Kannan V, Rymarquis LA, Nobuta K, German R, De Paoli E, Lu C, Schroth G, Meyers BC *et al.* (2008) **Global identification of microRNA-target RNA pairs by parallel analysis of RNA ends.** *Nat Biotech* **26**: 941-946
22. Johnson NR, Yeoh JM, Coruh C, Axtell MJ. (2016) **Improved placement of multi-mapping small RNAs.** *G3: Genes/Genomes/Genetics* **6**: 2103-2111
23. Guo QL, Qu XF, Jin WB. (2015) **PhaseTank: genome-wide computational identification of phasiRNAs and their regulatory cascades.** *Bioinformatics* **31**: 284-286
24. Anders S, Huber W. (2010) **Differential expression analysis for sequence count data.** *Genome Biol* **11**: R106
25. Meyers BC, Axtell MJ, Bartel B, Bartel DP, Baulcombe D, Bowman JL, Cao X, Carrington JC, Chen XM, Green PJ, Griffiths-Jones S, Jacobsen SE, Mallory AC, Martienssen RA *et al.* (2008) **Criteria for annotation of plant microRNAs.** *Plant Cell* **20**: 3186-3190
26. Dai X, Zhao PX. (2011) **psRNATarget: a plant small RNA target analysis server.** *Nucl Acids Res* **39**: W155-W159

27. Jagadeeswaran G, Saini A, Sunkar R. (2009) **Biotic and abiotic stress down-regulate miR398 expression in Arabidopsis.** *Planta* **229**: 1009-1014
28. Gou J-Y, Felippes FF, Liu C-J, Weigel D, Wang J-W. (2011) **Negative regulation of anthocyanin biosynthesis in Arabidopsis by a miR156-targeted SPL transcription factor.** *Plant Cell* **23**: 1512-1522
29. Zhang H, Zhao X, Li J, Cai H, Deng XW, Li L. (2014) **MicroRNA408 is critical for the HY5-SPL7 gene network that mediates the coordinated response to light and copper.** *Plant Cell* **26**: 4933-4953
30. Gielen H, Remans T, Vangronsveld J, Cuypers A. (2016) **Toxicity responses of Cu and Cd: the involvement of miRNAs and the transcription factor SPL7.** *BMC Plant Biol* **16**: 145
31. Brousse C, Liu Q, Beauclair L, Deremetz A, Axtell MJ, Bouché N. (2014) **A non-canonical plant microRNA target site.** *Nucl Acids Res* **42**: 5270-5279
32. Pimentel H, Bray NL, Puente S, Melsted P, Pachter L. (2017) **Differential analysis of RNA-seq incorporating quantification uncertainty.** *Nat Meth* **14**: 687-690
33. Pinweha N, Asvarak T, Viboonjun U, Narangajavana J. (2015) **Involvement of miR160/miR393 and their targets in cassava responses to anthracnose disease.** *J Plant Physiol* **174**: 26-35
34. Zhang XM, Zhao HW, Gao S, Wang WC, Katiyar-Agarwal S, Huang HD, Raikhel N, Jin HL. (2011) **Arabidopsis Argonaute 2 regulates innate immunity via miRNA393*-mediated silencing of a Golgi-localized SNARE gene, MEMB12.** *Mol Cell* **42**: 356-366
35. Navarro L, Dunoyer P, Jay F, Arnold B, Dharmasiri N, Estelle M, Voinnet O, Jones JDG. (2006) **A plant miRNA contributes to antibacterial resistance by repressing auxin signaling.** *Science* **312**: 436-439
36. Llave C, Xie ZX, Kasschau KD, Carrington JC. (2002) **Cleavage of Scarecrow-like mRNA targets directed by a class of Arabidopsis miRNA.** *Science* **297**: 2053-2056
37. Rock CD. (2013) **Trans-acting small interfering RNA4: key to nutraceutical synthesis in grape development?** *Trends Plant Sci* **18**: 601-610
38. Klevebring D, Street N, Fahlgren N, Kasschau K, Carrington J, Lundeberg J, Jansson S. (2009) **Genome-wide profiling of Populus small RNAs.** *BMC Genomics* **10**: 620
39. Lin J-S, Lin C-C, Lin H-H, Chen Y-C, Jeng S-T. (2012) **MicroR828 regulates lignin and H₂O₂ accumulation in sweet potato on wounding.** *New Phytol* **196**: 427-440
40. Xia R, Zhu H, An Y-q, Beers E, Liu Z. (2012) **Apple miRNAs and tasiRNAs with novel regulatory networks.** *Genome Biol* **13**: R47
41. Zhu H, Xia R, Zhao BY, An YQ, Dardick CD, Callahan AM, Liu ZR. (2012) **Unique expression, processing regulation, and regulatory network of peach (*Prunus persica*) miRNAs.** *BMC Plant Biol* **12**: 18
42. Zhai J, Jeong D-H, De Paoli E, Park S, Rosen BD, Li Y, Gonzalez AJ, Yan Z, Kitto SL, Grusak MA, Jackson SA, Stacey G, Cook DR, Green PJ *et al.* (2011) **MicroRNAs as master regulators of the plant NB-LRR defense gene family via the production of phased, trans-acting siRNAs.** *Genes Dev* **25**: 2540-2553
43. Zhang C, Li G, Wang J, Fang J. (2012) **Identification of trans-acting siRNAs and their regulatory cascades in grapevine.** *Bioinformatics* **28**: 2561-2568
44. Guan X, Pang M, Nah G, Shi X, Ye W, Stelly DM, Chen ZJ. (2014) **miR828 and miR858 regulate homoeologous MYB2 gene functions in Arabidopsis trichome and cotton fibre development.** *Nat Commun* **5**: 3050
45. Källman T, Chen J, Gyllenstrand N, Lagercrantz U. (2013) **A significant fraction of 21 nt sRNA originates from phased degradation of resistance genes in several perennial species.** *Plant Physiol* **162**: 741-754
46. Xia R, Xu J, Arikait S, Meyers BC. (2015) **Extensive families of miRNAs and PHAS loci in Norway spruce demonstrate the origins of complex phasiRNA networks in seed plants.** *Mol Biol Evol* **32**: 2905-2918
47. Pantaleo V, Szittya G, Moxon S, Miozzi L, Moulton V, Dalmay T, Burgyan J. (2010) **Identification of grapevine microRNAs and their targets using high-throughput sequencing and degradome analysis.** *Plant J* **62**: 960-976
48. Turner M, Yu O, Subramanian S. (2012) **Genome organization and characteristics of soybean microRNAs.** *BMC Genomics* **13**: 169
49. Shivaprasad PV, Chen HM, Patel K, Bond DM, Santos B, Baulcombe DC. (2012) **A microRNA superfamily regulates nucleotide binding site-leucine-rich repeats and other mRNAs.** *Plant Cell* **24**: 859-874
50. Xia R, Meyers BC, Liu Z, Beers EP, Ye S, Liu Z. (2013) **MicroRNA superfamilies descended from miR390 and their roles in secondary small interfering RNA biogenesis in Eudicots.** *Plant Cell* **25**: 1555-1572

51. Li F, Pignatta D, Bendix C, Brunkard JO, Cohn MM, Tung J, Sun H, Kumar P, Baker B. (2012) **MicroRNA regulation of plant innate immune receptors.** *Proc Natl Acad Sci U S A* **109**: 1790-1795
52. Jackson LK, Joyce RJ, Laikhtman M, Jackson PE. (1998) **Determination of trace level bromate in drinking water by direct injection ion chromatography.** *J Chromatog A* **829**: 187-192
53. Roberts JKM. (1984) **Study of plant metabolism in vivo using NMR spectroscopy.** *Annu Rev Plant Physiol* **35**: 375-386
54. Wallis CM, Chen J. (2012) **Grapevine phenolic compounds in xylem sap and tissues are significantly altered during infection by *Xylella fastidiosa*.** *Phytopathology* **102**: 816-826
55. Wallis CM, Wallingford AK, Chen J. (2013) **Grapevine rootstock effects on scion sap phenolic levels, resistance to *Xylella fastidiosa* infection, and progression of Pierce's disease.** *Front Plant Sci* **4**: 502
56. Wallis CM, Wallingford AK, Chen J. (2013) **Effects of cultivar, phenology, and *Xylella fastidiosa* infection on grapevine xylem sap and tissue phenolic content.** *Physiol Mol Plant Pathol* **84**: 28-35
57. Jacobs T, LaFayette P, Schmitz R, Parrott W. (2015) **Targeted genome modifications in soybean with CRISPR/Cas9.** *BMC Biotechnol* **15**: 16
58. Mali P, Yang L, Esvelt KM, Aach J, Guell M, DiCarlo JE, Norville JE, Church GM. (2013) **RNA-guided human genome engineering via Cas9.** *Science* **339**: 823-826